



# Dielectric properties of silicon nitride ceramics produced by free sintering



O.A. Lukianova\*, V.V. Sirota

Belgorod National Research University, Center of the Structural Ceramics and Engineering Prototyping, 85, Pobedy Str., 308015 Belgorod, Russia

## ARTICLE INFO

### Keywords:

Silicon nitride  
Dielectric losses  
Sintering

## ABSTRACT

The silicon nitride ceramics with a beneficial combination of low dielectric losses and improved physical properties was fabricated by cold isostatic pressing and pressureless sintering. The fine grain microstructure, three-phase composition based on the  $\beta$ -SiAlON, the small amount of the glass phase and relatively small porosity promote a unique combination of a low thermal conductivity  $14.51 \text{ W m}^{-1} \text{ K}^{-1}$  and low dielectric loss  $1.4 \cdot 10^{-3}$ . A novel method is proposed to overcome the main drawbacks of the commercial and high-cost technologies.

## 1. Introduction

The high performance silicon nitride ceramics has a great potential for aircraft and aerospace industry applications. An attractive combination of high strength, high oxidation resistance and low dielectric losses makes the silicon nitride ceramics interesting for a wide range of technical, industry and structural applications, such as gas turbine engines, next-generation power devices, turbocharger rotors, microwave devices and diesel engine components [1]. However, these properties typically have opposing characteristics, e.g., silicon nitride may be strong or exhibit low dielectric losses, but they are rarely both. The low dielectric losses of  $\text{Si}_3\text{N}_4$  also make it a promising alternative candidate for the aviation and aerospace industry, namely, rocket production, antenna window and high speed missile radomes, the electrical insulators for a fusion powers reactor, such composite elements as aircraft missile, both front edges, missile warheads (nose cone) and the nozzle sleeve rocket engines, radio-windows, etc.

Common sintering additives are mixtures of such metal oxides as aluminum oxide, yttrium oxide and magnesium oxide. The most promising processing methods, which allow us the fabrication of advanced silicon nitride ceramics with improved mechanical properties, involve cold isostatic pressing (CIP) and pressureless sintering. It is well known, that the porosity in silicon nitride can be easily removed by such commercial methods as hot isostatic pressing (HIP) and spark plasma sintering (SPS). HIPed silicon nitride has substantially higher strength and ultimate tensile strengths with high levels of damage tolerance. To overcome the economic limitations of HIP and SPS, a process of cold isostatic pressing with a free low temperature and fast sintering was developed for application in the rocket industry. Due to the possibility of obtaining of complex shape and large size products

the investigated method can be used as an economically and functionally superior alternative to other types of commercial methods. The proposed method can greatly reduce the cycle time to 60 min. As a result, this process can be applied for mass production.

At the same time, the dielectric constant and the dielectric loss tangent are the key factors for radiopacity of ceramics. Porous  $\text{Si}_3\text{N}_4$  ceramics have been developed to decrease the dielectric constant. In order to maintain high strength with low dielectric losses, it is desired to obtain fine grain microstructure and uniformly distributed small pores. It is one of the primary concerns in the processing of  $\text{Si}_3\text{N}_4$  ceramics.

Thus, the main aims of the presented work are to report dielectric and physical properties of the pressureless sintered silicon nitride ceramics and to compare the mechanical and dielectric properties of silicon nitrides produced by different methods.

## 2. Material and methods

The initial  $\text{Si}_3\text{N}_4$  powder was  $\alpha$ -rich  $\text{Si}_3\text{N}_4$  (Stark, Grade M11) with particle size of 600 nm with a high purity and high specific surface area.  $\text{Y}_2\text{O}_3$  (Stark, Grade, 2  $\mu\text{m}$ ) and  $\text{Al}_2\text{O}_3$  (A16 SG, 600 nm) sintering additives were used as starting materials. The mixture of powders was milled in the vibratory disc mill Retsch RS-200 for 20 min and, then, cold isostatically pressed at 200 MPa. Samples were heated using a constant heat rate of 25  $^\circ\text{C min}$  and sintered at 1650  $^\circ\text{C}$ , in a Nabertherm VHT 8 22-GR furnace under 0.1 MPa nitrogen pressure and using a silicon nitride powder bed. Other material and processing details were reported in previous work [2–4].

The dielectric loss tangent and permittivity were carried out using ET-1 device with OBR-1 and MDR-1 resonators in the temperature

\* Corresponding author.

E-mail address: [sokos100@mail.ru](mailto:sokos100@mail.ru) (O.A. Lukianova).

range from 20 to 400 °C at 9 GHz.

Experimental samples were cut with a band saw from a sintered billet. One specimen from the batch was examined in a transmission electron microscope (JEOL-2100) at 200 kV. Foils for TEM were prepared from slices hand ground and finally ion-polished until perforation. Structural characterization was performed using scanning electron microscope and Quanta 600 FEG (FEI Company, Hillsboro, OR).

### 3. Theory

The molar heat capacity of produced ceramics was calculated by the Debye theory. The Debye temperature  $\theta_D$  was calculated according to the following equation [5]:

$$\theta_D = \frac{h}{k_B} \left( \frac{9N}{4\pi V} \right)^{1/3} \cdot \left( \frac{1}{v_l^3} + \frac{2}{v_t^3} \right)^{-1/3} \quad (1)$$

where  $h$  is the Planck's constant,  $k_B$  is the Boltzmann's constant,  $N/V$  is the atomic concentration,  $8.6 \cdot 10^{28}$  atoms/m<sup>3</sup>,  $v_l$  is the longitudinal sound velocity,  $v_t$  is the transverse sound velocity.  $v_l$  and  $v_t$  were calculated as follows:

$$v_l = \sqrt{\frac{E(1-\nu)}{\rho(1-2\nu)(1+\nu)}} \quad (2)$$

$$v_t = \sqrt{\frac{G}{\rho}} \quad (3)$$

where  $G$  is the shear modulus,  $E$  is the Young's modulus,  $\rho$  is the material density and  $\nu$  is the Poisson's ratio.

The elastic properties of the investigated material were measured by the resonance method and described in our previous work [2].

The molar isochoric heat capacity was calculated as follows [6]:

$$C_V = 3R \left[ 4D(x) - \frac{3x}{e^x - 1} \right] \quad (4)$$

where  $R$  is the molar gas constant,  $x$  is  $\theta_D/T$  ratio ( $T$  is the temperature), and  $D(x)$  is the Debye function:

$$D(x) = \frac{3}{x^3} \int_0^x \frac{\xi^3}{e^\xi - 1} d\xi \quad (5)$$

This function was approximated by the sixth-degree polynomial by the least squares method.

The isochoric  $c_p$  heat capacity was described via the well-known relationship [7]:

$$c_p = c_v + V_m \cdot T \cdot \alpha_p^2 / K_T \quad (6)$$

where  $V_m$  is the molar volume,  $c_v$  is the molar heat capacity,  $\alpha_p$  is the coefficient of thermal expansion,  $K_T = 1/B_T$  is the isothermal compressibility coefficient.

The coefficient of thermal expansion was measured by Netzsch DIL 402C/4/G in temperature range of 20–900 °C.

The thermal diffusivity was measured by a laser flash method using a thermal constant analyzer LFA 457 Microflash Netzsch at room and elevated temperature from 20 to 500 °C. The thermal conductivity of the material can be estimated as:

$$k = \rho \cdot c_p \cdot \alpha \quad (7)$$

where  $k$  is the thermal conductivity, W/m K,  $\rho$  is the density kg/m<sup>3</sup>,  $c_p$ -specific heat, J/kg K.

### 4. Results

Fully dense SiAlON was obtained by cold isostatic pressing and free sintering. Fig. 1 shows a microstructure of a polished specimen. The microstructure generally consisted of large and small equiaxed grains

with a grain size distribution from 300 to 800 nm. The dielectric constant of the fabricated ceramics was 7.0 and the dielectric loss tangent was  $1.4 \cdot 10^{-3}$  at room temperature. The dielectric loss tangent and the dielectric constant are plotted in Fig. 2 as functions of the temperature. The complex permittivity and dissipation factor of the specimens increase with an increase in the temperature. In particular, the dielectric loss tangent increases with an increase in the temperature from 20 °C to 350 °C. The highest dielectric loss tangent was observed at 400 °C. Further increase in the testing temperature up to 500 °C is accompanied with an increase in the dielectric loss tangent. Some dielectric and mechanical properties of silicon nitride ceramics produced by different methods are presented in Table 1. Table 1 shows that the investigated ceramics had a high density and low surface porosity (0.1%) [2].

It can be noted that the present ceramics has moderately low thermal conductivity  $14.51 \text{ W m}^{-1} \text{ K}^{-1}$  and thermal diffusivity  $5.92 \text{ m}^2 \text{ s}^{-1}$  (Table 2).

The Debye temperature of the present material was 804 K (Table 3) according to the Eq. (1). Fig. 3 shows the curve of the heat capacity calculated for obtained ceramics according to the Debye theory.

### 5. Discussion

XRD of produced ceramics showed that the microstructure of this material consists of two main phases: the  $\alpha$  silicon nitride and  $\beta$ -SiAlON. By means of diffusion the fabricated ceramics featured such substitutional solid solutions as  $\beta$ -sialon  $\text{Si}_5\text{AlON}_7$  as well as a small amount of  $\text{Y}_2\text{SiAlON}_5$  (B-phase) [8]. The XRD analyses revealed  $\beta$ - $\text{Si}_5\text{AlON}_7$  ( $x=1$ ) as a major phase. It was reported that the SiAlON with  $x < 1.5$  are preferred as compared with the HIPed silicon nitride due to the lower dielectric losses [9]. The negative effect of MgO on the structure and physical properties in  $\text{Si}_3\text{N}_4$  ceramics was identified in our previous work [10,11]. It was associated with the recrystallization and high sintering temperature. The higher sintering temperature of silicon nitride with  $\text{Al}_2\text{O}_3$ -MgO is caused by the higher melting point of MgO (2852 °C) compared with the melting point of  $\text{Y}_2\text{O}_3$  (2425 °C). Also the dielectric loss tangent and dielectric permittivity of the MgO- $\text{Al}_2\text{O}_3$ - $\text{SiO}_2$  alkali-free glass systems increases strongly with the increase in the concentration of MgO in the microwave range [9]. Thus, such additives as  $\text{Al}_2\text{O}_3$ - $\text{Y}_2\text{O}_3$  eventually lead to the optimal complex of dielectric and mechanical properties of produced ceramics. Silicon nitride ceramics are frequently used as high-temperature dielectrics and therefore the electrophysical properties are crucial for such materials. Ohno et al. showed that the dielectric loss tangent of the MgO and  $\text{Al}_2\text{O}_3$ - $\text{Y}_2\text{O}_3$  doped silicon nitride was  $2 \cdot 10^{-3}$ – $4 \cdot 10^{-3}$  at room temperature at 9.1 GHz and increased significantly to  $10 \cdot 10^{-3}$ – $15 \cdot 10^{-3}$  with an increase in the temperature up to 800 °C [12]. It's obvious that the glass phase had a higher dielectric loss tangent compared with the HPSN (hot pressed silicon nitride), because silica and such other additives as  $\text{Ca}^{2+}$ ,  $\text{Al}^{3+}$ ,  $\text{Fe}^{2+}$ ,  $\text{Na}^+$  and  $\text{Cl}^-$  were generally used for the glass phase formation [13–15].

Dielectrical properties of ceramics essentially depend on the developed microstructure. Fig. 1 shows the microstructures of the sintered ceramics. The figure shows the typical structure of SiAlON (Fig. 1). This structure is mostly homogeneous.  $\text{Si}_3\text{N}_4$  particles with an essentially equiaxed hexagonal shape strongly dominate the material (Fig. 1). A low value of the dielectric loss tangent can be explained by the fine-grained microstructure consisting of fine equiaxed grains with the average size ranged from 0.3 to 0.8  $\mu\text{m}$  as can be seen clearly from the SEM studies (Fig. 1b). These results have a good correlation with a similar TEM microstructure results (Fig. 1a). The microstructure of the ceramics has been described in detail in previous works [8]. Park et al. showed that increase in the grain size led to increase in the dielectric properties of the magnesium, yttrium and aluminum oxide doped hot pressed silicon nitride ceramics and found that an increase in the grain size from 0.5 to 3.5  $\mu\text{m}$  led to increasing the  $\tan \delta$  from  $1 \cdot 10^{-3}$  to  $6 \cdot 10^{-3}$

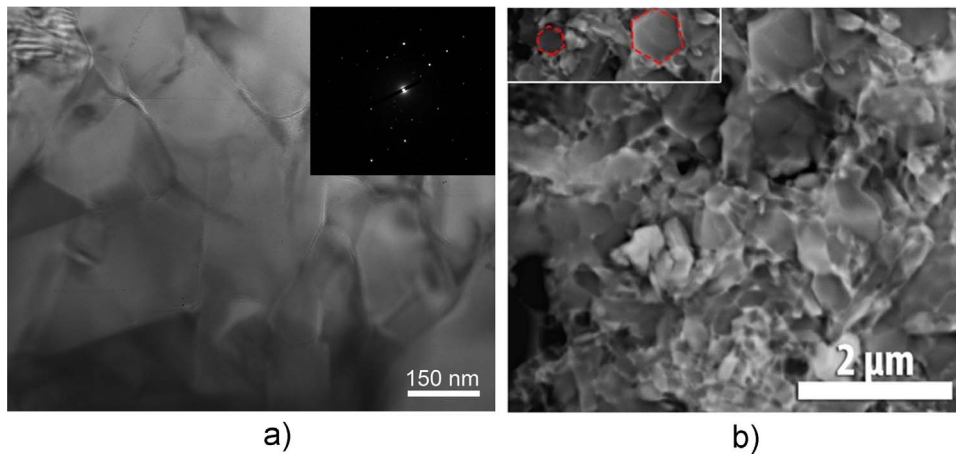


Fig. 1. Microstructure of the produced ceramics a) TEM b) SEM.

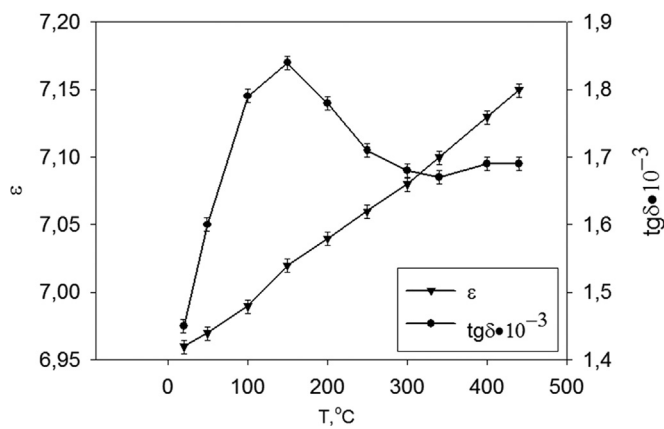


Fig. 2. Dielectric properties of the produced Si<sub>3</sub>N<sub>4</sub> ceramics.

[16]. The peak on the temperature loss tangent curve is due to the evaporation of the absorbed water. An increase in the value of the dielectric losses may be related to the conductivity. The intensity of displacement of charges increases with the heating of the dielectric in this case. Also, the dielectric loss may be associated with a polarization. This type of curve has a clearly marked maximum. It can be explained by the high viscosity and lack of losses at low temperature while the viscosity is low and the dipoles are moved without friction at high temperatures. Thus the observed curve is typical for this type of material (Fig. 2). The both ε and tan δ of RBSN practically do not increase with the temperature in the microwave range as it was shown in Ref. [9]. It was also noted that the dielectric losses in RBSN are largely determined by internal polarization at grain boundaries and phase boundaries [9].

The combination of high mechanical properties, low dielectric losses and excellent thermal shock resistance is quite important to ensure high radiopacity.

The most significant drawback of ceramics is the relatively low strength

Table 1

The dielectric properties of the silicon nitride ceramics produced by different methods.

g/cm <sup>3</sup>	Poros,%	Flex, MPa	Fq, HGz	ε	tan δ	Method	Ref.
1.3–2.0	–	60–180	8–18	2.3–3.4	1.6–2.5·10 <sup>-3</sup>	Sintering	[18]
–	16.2–42.6	47–112	1	3.1–4.5	2.6–4.3·10 <sup>-3</sup>	RB	[19]
2.84–2.97	–	310–320	4	7.3	3·10 <sup>-3</sup>	Sintering	[20]
–	–	57	–	2.8–3.1	–	Slurry vacuum infiltration	[21]
3.0–3.3	0–5	> 350	10	7.4 – 8.5	7·10 <sup>-3</sup>	HIP	[23]
2.5–2.7	10–16	> 200	10	6.1 – 6.6	15·10 <sup>-3</sup>	RB	[23]
2.97	0.1 (surf)	280	9	7.0	1.4·10 <sup>-3</sup>	CIP+sintering	This work

Table 2

Thermal properties.

C <sub>p</sub> , J/g K	α 10 <sup>-6</sup> , m <sup>2</sup> /s	k, W/m K
0.78	5.92	14.51

Table 3

Properties of the silicon nitride based ceramics.

	This work	[4]
Poisson's ratio, ν	0.28	–
Young's modulus, E, GPa	214	–
Shear modulus, G, GPa	90	–
Density, ρ, g/cm <sup>3</sup>	2.97	2.92
Longitudinal sound velocity, m/s · 10 <sup>3</sup>	9.6	9.1
Transverse sound velocity, m/s · 10 <sup>3</sup>	5.5	5.3
Atomic concentration, N/V, atoms/m <sup>3</sup> · 10 <sup>28</sup>	8.61	8.29
Debye temperature, θ <sub>D</sub> , K	804	763

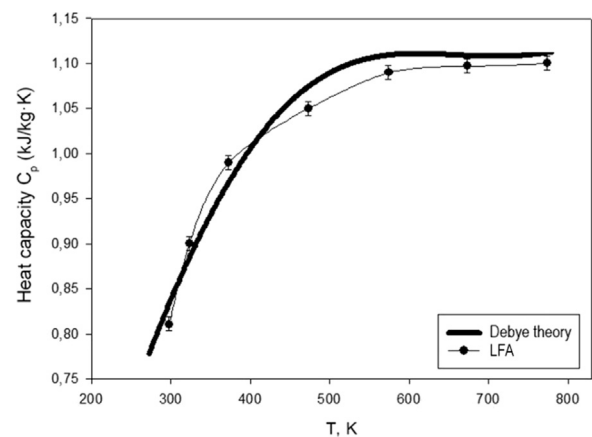


Fig. 3. High-temperature heat capacity for produced ceramics using θ<sub>D</sub>=804 K.

[17]. The reinforcing of ceramics by fibers and nanotubes leads to increasing of mechanical properties and to anisotropy at the same time. The temperature dependence of dielectric loss of investigated ceramics has correlation with mechanical properties. Particularly, the compression strength and the three-point bending strength change insignificantly in the temperature range of 20–350 °C as described in our previous work. The degradation in strength occurs at the same temperature of 350 °C where the dielectric losses saturated [2].

The permittivity change up to 450 °C temperature is not large and the temperature coefficient of permeability was very low and equal to  $4.7 \cdot 10^{-4} \text{ K}^{-1}$ . Porosity was relatively low (Table 1). It is obvious, that the permittivity and the strength of ceramics depend on porosity. It is well known that the complex permittivity depends on the porosity and can be expressed by a following relationship:

$$\varepsilon = \varepsilon_0^{1-P} \quad (8)$$

where  $\varepsilon_0$  is the permittivity of the 100% dense material and P is the percentage of pores. Thus, it is obvious that such methods as reaction bonding, low molding pressure, etc., lead to a high porosity and low permittivity. For instance, Wang et al. described silicon nitride fabricated by low molding and pressureless sintering. The flexural strength of  $\text{Si}_3\text{N}_4$  ceramics with 45–60% porosity was ranged from 57 to 176 MPa, the dielectric constant was 2.35–3.39, and the dielectric loss was  $1.6\text{--}3.5 \cdot 10^{-3}$  at 8–18 GHz (Table 1) [18]. Moreover, the reaction bonded silicon nitride had a rather high flexural strength 137 MPa, low dielectric constant 2.9 and dielectric loss tangent  $4.6 \cdot 10^{-3}$  at 1 GHz (Table 1) [19]. The calculated permittivity of the described ceramics according to formula (8) was equal to 6.7 and closely agrees with the experimental value. Interestingly, the value of the dielectric loss tangent of the present ceramics is one of the lowest dielectric loss data reported for the  $\text{Si}_3\text{N}_4$  ceramics. The presented material is also characterized by a better combination of mechanical and physical properties compared to the silica bonded porous silicon nitride ceramics fabricated by the oxidation bonding [19]. Particularly, the porosity of the reaction bonded (RB) silicon nitride ranged from 16.2% to 42.6%, the flexural strength varied from 47 MPa to 112 MPa depending on the sintering temperature, whereas, the density of the present silicon nitride was  $2.97 \text{ g/cm}^3$ , the surface porosity was 0.1%, the flexural strength was 275 MPa (see Table 1). The dielectric losses of the fabricated ceramics were also lower than for the reaction bonded ceramics (see Table 1). Barta et al. studied dielectric properties of the sintered silicon nitride ceramics. Although, Table 1 shows that the sintered ceramics exhibits slightly higher flexural strength (310–320 MPa) than the bending strength of the present ceramics, but, however, its dielectric properties are higher ( $\varepsilon=7.3$ ,  $\tan \delta=3 \cdot 10^{-3}$ ) compared with present ones [20]. Han et al. studied two-dimension fiber reinforced silicon nitride matrix composites with excellent dielectric constant  $\varepsilon=2.8\text{--}3.1$ , but low strength of 57 MPa and high porosity [21]. Changlian et al. reported that the  $\beta\text{-Si}_3\text{N}_4$  has a lower dielectric constant compared with  $\alpha\text{-Si}_3\text{N}_4$ . It was shown that the dielectric constant of the  $\text{Si}_3\text{N}_4$  with  $\text{Al}_2\text{O}_3$  and MgO produced by SPS ranged from 5.0 to 7.5, meanwhile, the density of this material varied between  $2.48\text{--}3.09 \text{ g/cm}^3$ . The density and dielectric constant are almost increased with an increase in the temperature and amount of additives [22]. Suzdaltsev et al. reported the dielectric loss tangent of the hot pressed silicon nitride varied from 7.4 to 8.5, while the dielectric loss tangent of the reaction bonded silicon nitride ranged from 6.1 to 6.6 (see Table 1) [23]. It is obvious that both methods have limitations and disadvantages. However, the proposed method is cheaper than HIP. ShuQin et al. described dielectric properties of porous  $\text{Si}_2\text{N}_2\text{O}\text{--}\text{Si}_3\text{N}_4$  composites fabricated by gel-casting with a flexural strength of 231 MPa. The complex permittivity of the composites varied from 4.3 to 4.6 and the dissipation factor ranged from 0.5 to  $1.0 \cdot 10^{-3}$  (Table 1) [24].

Miyazaki et al. described the hot isostatic pressed silicon nitride with a dielectric constant ranged from 6.3 to 7.2. The  $\tan \delta$  of this ceramics with 2 mol% of  $\text{Yb}_2\text{O}_3$  and 7 mol% of  $\text{SiO}_2$  was decreased significantly to  $3 \cdot 10^{-4}$  after annealing. No change was observed for 0.5 mol% of  $\text{Yb}_2\text{O}_3$  and 11.5 mol% of  $\text{SiO}_2$  sample. The same value of

the dielectric constant as obtained in the present study have been observed for  $\text{Si}_3\text{N}_4$  ceramics sintered at 1900 °C for 3 h. The dielectric constant of  $\text{Si}_3\text{N}_4$  ceramics was 7.1–7.2 before annealing and 6.3–6.4 after annealing at 2 GHz [25]. The dielectric losses of produced ceramics are lower than the dielectric losses of commercial silicon nitride called IRBAS and Ceralloy [26].

Thus the obtained material exhibits higher mechanical performance than the reaction bonding ceramics and lower dielectric losses comparing to the HIPed ceramics. The Debye temperature of produced ceramics is in accordance with results presented by Watari et al. (Table 3) [5].

Silicon nitride with a low thermal conductivity is preferable for the manufacture of radomes. However Hagerty and Lighfoot suggested a high thermal conductivity of the silicon nitride ranging from 200 to  $320 \text{ W m}^{-1} \text{ K}^{-1}$  [27]. The hot pressed silicon nitride with beryllium oxide and high thermal conductivity was also reported [28]. Hirao et al. described the high thermal conductivity of  $120 \text{ W m}^{-1} \text{ K}^{-1}$  and anisotropy of the hot pressed silicon nitride ceramics [29]. There is known  $\text{MgSiN}_2$  doped ceramics with a high thermal conductivity  $100 \text{ W m}^{-1} \text{ K}^{-1}$  [30]. Okamoto et al. and Hayashi et al. described the magnesium oxide doped silicon nitride with high thermal conductivity  $128 \text{ W m}^{-1} \text{ K}^{-1}$  produced by the gas pressure sintering [31,32]. This type of ceramics with yttrium and aluminum oxides has a thermal conductivity in the range from 40 to  $70 \text{ W m}^{-1} \text{ K}^{-1}$  and a nearly full density [31].

For comparison, Corral et al. described the SPSed  $\text{Si}_3\text{N}_4$  and SWNT- $\text{Si}_3\text{N}_4$  (single-walled carbon nanotubes) nanocomposites with relatively low thermal conductivity from 5.22 to  $27.70 \text{ W m}^{-1} \text{ K}^{-1}$  while the thermal diffusivity varied from  $3.7 \cdot 10^{-6}$  to  $13.6 \cdot 10^{-6} \text{ m}^2 \text{ s}^{-1}$  according to the content of the single-walled carbon nanotubes [33]. Dong et al. also presented different types of  $\beta\text{-SiAlON}$  with low value of thermal conductivity  $5.56\text{--}16.48 \text{ W m}^{-1} \text{ K}^{-1}$  and thermal diffusivity  $2.0\text{--}6.5 \cdot 10^{-6} \text{ m}^2 \text{ s}^{-1}$  [34].

## 6. Conclusions

In summary low loss tangent and low thermal conductivity silicon nitride ceramics  $\text{Al}_2\text{O}_3\text{--}\text{Y}_2\text{O}_3$  doped with a high content of aluminum oxide have been prepared by cold isostatic pressing and pressureless sintering. Due to the rapid pressureless sintering the proposed technology can provide a powerful, cheap and rapid method for the fabrication of  $\text{Si}_3\text{N}_4$  ceramics. The main results can be summarized as follows:

1. The dielectric loss tangent was  $1.4 \cdot 10^{-3}$  at room temperature.
2. The heat capacity calculated by the Debye theory was  $0.78 \text{ J/g K}$  and the Debye temperature was 804 K.
3. The thermal conductivity was  $14.5 \text{ W m}^{-1} \text{ K}^{-1}$  and thermal diffusivity was  $5.92 \cdot 10^{-6} \text{ m}^2/\text{s}$ .

## Acknowledgements

The financial support received from the RFBR according to the research project No. 16-32-00430 mol\_a is gratefully acknowledged. The authors are grateful to the personnel of the East-Siberian Branch of Federal State Unitary Enterprise "National Research Institute of Physico-Technical and Radio Engineering Measurements" and Advanced Ceramics Group for their assistance with instrumental analysis.

## References

- [1] A. Hosneara, A.H. Hasnat, Bhuyan, Structural and electrical properties of reaction bonded silicon nitride ceramics, *Open Ceram. Sci. J.* 2 (2012) 1–7.
- [2] O. Lukianova, Mechanical and elastic properties of new silicon nitride ceramics produced by cold isostatic pressing and free sintering, *Ceram. Int.* 41 (2015) 13716–13720.
- [3] V.V. Krasil'nikov, V.V. Sirotina, A.S. Ivanov, L.N. Kozlova, O.A. Luk'yanova, V.V. Ivanisenko, Investigation of the structure of  $\text{Si}_3\text{N}_4$ -based ceramic with  $\text{Al}_2\text{O}_3$  and  $\text{Y}_2\text{O}_3$  additives, *Glass Ceram.* 71 (2014) 15–17.
- [4] V. Sirotina, V. Krasil'nikov, O. Lukianova, Fabrication of the ceramics based on silicon nitride by free sintering and cold isostatic pressing, *NANOCON 2013—Conference Proceedings, 5th International Conference, 2013*. pp. 248–251.

- [5] K. Watari, Y. Seki, K. Ishizaki, temperature dependence of thermal coefficients for HIPped silicon nitride, *J. Ceram. Soc. Jpn.* 97 (1989) 174–181.
- [6] T.W. Listerman, C.B. Ross, Cryogenics (Guildf). A simple method for calculating Debye heat capacity values using the Einstein heat capacity formula, *Cryogenics* 19 (1979) 547–549.
- [7] M. Abramowitz, I.A. Stegun, *Handbook of Mathematical Functions: With Formulas, Graphs, and Mathematical Tables*, Tenth, National Bureau of Standards, Washington, 1972.
- [8] O.A. Lukianova, V.V. Krasilnikov, A.A. Parkhomenko, V.V. Sirota, Microstructure and phase composition of cold isostatically pressed and pressureless sintered silicon nitride, *Nanoscale Res. Lett.* 11 (2016) 148.
- [9] T.Ya. Kosolapova, T.V. Andreeva, T.S. Bartnitskaya, G.G. Gnesin, G.N. Makarenko, I.I. Osipova, E.V. Prilutskiy, Non-metallic refractory compounds, *Metallurgy*, Moscow, 1985, p.224.
- [10] V. Sirota, O. Lukianova, V. Krasilnikov, V. Selemenev, V. Dokalov, Microstructural and physical properties of magnesium oxide-doped silicon nitride ceramics, *Res. Phys.* 6 (2016) 82–83.
- [11] O.A. Lukianova, V.V. Sirota, V.V. Krasilnikov, A.A. Parkhomenko, Mechanical properties and microstructure of silicon nitride fabricated by pressureless sintering, in: *Proceedings of International Conference on Nanomaterials: Application & Properties (NAP)*, 2016, 02NSA09-1–02NSA09-3.
- [12] H. Ohno, Y. Katano, Electrical properties of silicon nitride, *Mater. Sci. Forum* 47 (1989) 215–227.
- [13] D.R. Clarke, High temperature environmental strength degradation of a hot-pressed silicon nitride: an experimental test, *J. Am. Ceram. Soc.* 66 (1983) 156–158.
- [14] D.R. Clarke, G. Thomas, Microstructure of YO fluxed hot-pressed silicon nitride, *J. Am. Ceram. Soc.* 61 (1978) 114–118.
- [15] D.R. Clarke, N.J. Zaluzec, R.W. Carpenter, The intergranular phase in hot-pressed silicon nitride: 11. Evidence for phase separation and crystallization, *J. Am. Ceram. Soc.* 64 (1981) 608–611.
- [16] M.K. Park, H.N. Kim, K.S. Lee, S.S. Baek, E.S. Kang, Y.K. Baek, D.K. Kim, Effect of Microstructure on Dielectric Properties of Si<sub>3</sub>N<sub>4</sub> at Microwave Frequency, *Key Eng. Mater.* 287 (2005) 247–252.
- [17] J. Ning, J. Zhang, Y. Pan, J. Guo, Fabrication and mechanical properties of SiO<sub>2</sub> matrix composites reinforced by carbon nanotube, *Mater. Sci. Eng. A* 357 (2003) 392–396.
- [18] H. Wang, J. Yu, J. Zhang, D.J. Zhang, Preparation and properties of pressureless-sintered porous Si<sub>3</sub>N<sub>4</sub>, *Mater. Sci.* 45 (2010) 3671–3676.
- [19] S. Ding, Y.-P. Zeng, D. Jiang, Oxidation bonding of porous silicon nitride ceramics with high strength and low dielectric constant, *Mater. Lett.* 61 (2007) 2277–2280.
- [20] J. Barta, M. Manela, R. Fischer, Si<sub>3</sub>N<sub>4</sub> and Si<sub>2</sub>N<sub>2</sub>O for high performance radomes, *Mater. Sci. Eng.* 71 (1985) 265–272.
- [21] G. Han, L. Zhang, L. Cheng, Processing and performance of 2D fused-silica fiber reinforced porous Si<sub>3</sub>N<sub>4</sub> matrix composites, *J. Univ. Sci. Technol. Beijing Miner. Metall. Mater.* 15 (2008) 58–61.
- [22] C. Changlian, C. Fei, S. Qiang, Z. Lianmeng, Y. Faqiang, Liquid phase sintering (LPS) and dielectric constant of  $\alpha$ -silicon nitride ceramic, *J. Wuhan Univ. Technol. Mater. Sci. Ed.* (2006) 98–100.
- [23] E.I. Suzdal'tsev, D.V. Kharitonov, A.A. Anashkina, Analysis of existing radioparent refractory materials, composites and technology for creating high-speed rocket radomes, *Refract. Ind. Ceram.* 51 (2010) 202–205.
- [24] L. ShuQin, P. YuChen, Y. ChangQing, L. JiaLu, Mechanical and dielectric properties of porous Si<sub>2</sub>N<sub>2</sub>O–Si<sub>3</sub>N<sub>4</sub> in situ composites, *Ceram. Int.* 35 (2009) 1851–1854.
- [25] H. Miyazaki, Y.-I. Yoshizawa, K. Hirao, Effect of crystallization of intergranular glassy phases on the dielectric properties of silicon nitride ceramics, *Mater. Sci. Eng. B* 148 (2008) 257–260.
- [26] ([http://viam-works.ru/ru/articles?art\\_id=957](http://viam-works.ru/ru/articles?art_id=957)).
- [27] J.S. Haggerty, A. Lightfoot, Opportunity for the enhancing the thermal conductivity of SiC and Si<sub>3</sub>N<sub>4</sub> ceramics through improved processing, *Ceram. Eng. Sci. Proc.* 16 (1995) 475–487.
- [28] N. Hirotsaki, Y. Okamoto, M. Ando, F. Munakata, Y. Akimune, Thermal conductivity of gas-pressure-sintered silicon nitride, *J. Am. Ceram. Soc.* 79 (1996) 2878–2882.
- [29] K. Hirao, K. Watari, M.E. Brito, M. Toriyama, S. Kanzaki, High thermal conductivity in silicon nitride with anisotropic microstructure, *J. Am. Ceram. Soc.* 79 (1996) 2485–2488.
- [30] G. Peng, M. Liang, Z. Liang, Q. Li, Spark plasma sintered silicon nitride ceramics with high thermal conductivity using MgSiN<sub>2</sub> as additives, *J. Am. Ceram. Soc.* 92 (2009) 2122–2124.
- [31] Y. Okamoto, N. Hirotsaki, M. Ando, F. Munakata, Y. Akimune, Effect of sintering additive composition on the thermal conductivity of silicon nitride, *J. Mater. Res.* 13 (1998) 3473–3477.
- [32] H. Hayashi, K. Hirao, M. Toriyama, S. Kanzaki, K. Itatani, MgSiN<sub>2</sub> addition as a means of increasing the thermal conductivity of  $\beta$ -silicon nitride, *J. Am. Ceram. Soc.* 84 (2001) 3060–3062.
- [33] E.L. Corral, H. Wang, J. Garay, Z. Munir, E.V. Barrera, Effect of single-walled carbon nanotubes on thermal and electrical properties of silicon nitride processed using spark plasma sintering, *J. Eur. Ceram. Soc.* 31 (2011) 391–400.
- [34] P.L. Dong, X.D. Wang, M. Zhang, S. Seshadri, Conductivity properties of  $\beta$ -SiAlON ceramics, *Sci. China Technol. Sci.* 55 (2012) 2409–2415.